Advanced Physical Research
Vol.8, No.1, 2026, pp.14-21
https://doi.org/10.62476/apr.8114

Jomard Publishing

INFLUENCE OF COOLING RATE ON STRUCTURAL AND ELECTROPHYSICAL CHANGES IN ZIRCONIUM-DOPED SILICON

Sharifa Utamuradova, Shokhrukh Daliyev, Shuhratbek Ismoilov*, Aysara Uteniyazova

Research Institute of Semiconductor Physics and Microelectronics, National University of Uzbekistan, Tashkent, Uzbekistan

Abstract. An experimental study was carried out to investigate the influence of cooling rate after high-temperature annealing on the structural and electrophysical properties of zirconium-doped p- and n-type silicon prepared by the diffusion method. Raman and FTIR spectroscopy were employed to assess crystalline quality, defect-related disorder, and oxygen-related bonding environments associated with zirconium incorporation. Electrophysical parameters, including resistivity (ρ), carrier concentration (n), and mobility (μ), were measured using the Hall method at 300 K. Rapid cooling was found to promote the preservation of electrically active zirconium-related states, resulting in reduced resistivity and enhanced carrier concentration and mobility, whereas slow cooling favors defect equilibration and structural stabilization. Arrhenius analysis of resistivity yielded shallow donor activation energies of approximately 0.05–0.06 eV, consistent with donor-like states introduced by zirconium. The temperature dependence of carrier mobility exhibits a weak sensitivity to temperature, indicative of scattering-limited transport rather than thermally activated carrier motion. Optimal processing conditions - annealing at approximately 1100 °C followed by rapid cooling - yield minimum resistivity ($\rho \approx 2\ \Omega \cdot$cm) and high mobility ($\mu \approx 900$ cm^2/V$\cdot$s). These results demonstrate the potential of zirconium-modified silicon for thermally stable sensor structures and microelectronic applications.

Keywords: activation energy, annealing, FTIR, Raman spectroscopy, silicon, zirconium.
Corresponding author: Shuhratbek Ismoilov, Research Institute of Semiconductor Physics and Microelectronics, National University of Uzbekistan, Tashkent, Uzbekistan, e-mail: *ismoilov-2015@inbox.ru*
Received: 27 November 2025; Revised: 28 December 2025; Accepted: 5 January 2026; Published: 18 February 2026.

1 Introduction

Silicon remains the fundamental material of modern micro- and nanoelectronics due to its well-developed technology, high purity, and ability to precisely control doping. However, further integration and miniaturization of the devices increase the requirements for material stability and dielectric properties. One of the effective ways to enhance the functionality of silicon structures is their modification with elements possessing a high dielectric constant, mainly zirconium and its oxides (Wilk et al., 2001; Robertson, 2006; Zhao et al., 2018). Compounds based on ZrO_2 exhibit a high dielectric constant ($\varepsilon \approx 25 - 30$), a wide band gap ($E_g \approx 5.5\ eV$), excellent thermal stability, and chemical inertness with respect to silicon (Xu et al., 2022; Wang et al., 2023; Ahn & Lee, 2020). This makes them promising as gate dielectrics, buffer, and passivation layers in MOS structures and high-temperature sensors. Studies by Robertson (2006) and Wilk et al. (2001) demonstrated that zirconium oxide can form thermally stable interfaces with silicon, ensuring a low density of surface traps. The works of Zhao et al. (2018) and Xu et al. (2022)

showed that thermal treatment in the range of $700-1100\ ^0C$ causes the phase evolution of ZrO_2 from amorphous to monoclinic and tetragonal structures, affecting electrophysical properties. Among the technological parameters, the cooling rate after annealing plays a crucial role in determining the degree of crystallinity and the concentration of defects in the material (Wang et al., 2023; Ahn & Lee, 2020; Cho, Park & Kim, 2021; Liu, Zhou & Zhang, 2022).

The cooling rate affects the distribution of zirconium impurities, the formation of oxide phases, and the creation of defect complexes. During slow cooling (together with the furnace), internal stress relaxation and grain growth occur, leading to structure stabilization but possibly causing the enlargement of ZrO_2 phases and a decrease in active donor concentration (Kim & Choi, 2023; Kato & Ito, 2020; Lee & Hwang, 2025). Rapid cooling (quenching) freezes metastable states, prevents zirconium atom aggregation, and helps maintain an increased concentration of electron donors (Sun & Li, 2021; Park & Lim, 2024; Chen & Zhang, 2023). Thus, changing the cooling rate after annealing is an effective tool for controlling the defect structure and electrophysical properties of $Si+Zr$. These effects are most pronounced at temperatures between $900\ ^0C$ and $1200\ ^0C$, where Zr diffusion becomes active and stable $Zr-O-Si$ complexes are formed (Kang & Yoo, 2019; Li & Yuan, 2020; Nakamura & Tanaka, 2019).

In the literature, zirconium has been reported to occupy interstitial and substitutional positions in the silicon lattice, forming donor-like centers with activation energies of $\sim 0.05-0.07\ eV$ (Patel & Singh, 2022). These levels contribute to an increase in carrier concentration n and mobility μ under appropriate thermal treatment conditions. Studies by Park & Lim (2024); Chen & Zhang (2023) and Lee & Hwang (2025) have shown that the formation of metastable states Zr near the conduction band enhances electronic conductivity. FTIR and Raman analyses carried out by Liu *et al.* indicate that the appearance of bands in the $960-1100\ cm^{-1}$ and $520\ cm^{-1}$ regions corresponds to the formation of $Si-O-Zr$ bonds and improved crystallinity. An important complement to the structural analysis is the temperature-dependent study of electrophysical characteristics-$\rho(T)$, $n(T)$, and $\mu(T)$-along with Arrhenius plots ($\ln\rho$-$1/T$, $\ln n$-$1/T$), which allow the determination of donor activation energies (Yamamoto & Saito, 2024; Morales & Diaz, 2025). Despite extensive studies of ZrO_2-based dielectrics, the effect of cooling rate on donor activation and electrophysical parameters of $Si+Zr$ has not yet been explored sufficiently. Therefore, a detailed investigation of temperature dependencies and the construction of energy models that consider the cooling effect after zirconium diffusion is of great current relevance.

Although cooling-rate effects after annealing have been discussed for silicon doped with conventional impurities, the role of post-annealing cooling in governing *zirconium-specific* electrically active configurations in silicon has not been systematically established. In zirconium-doped silicon, the cooling rate can control the stabilization or relaxation of oxygen-related $Si-O-Zr$ complexes, which directly impacts donor activation, compensation effects in p-type material, and transport parameters. The present study provides a comparative investigation of slow furnace cooling ($2-3\ ^0C/min$) versus rapid quenching ($>100\ ^0C/s$) after zirconium diffusion annealing ($700-1200\ ^0C$), and correlates structural signatures (Raman/FTIR) with electrophysical characteristics (ρ, n, μ) and activation energies. This approach enables identification of an optimal technological window (annealing near $1100\ ^0C$ followed by rapid quenching) for achieving simultaneously low resistivity and high mobility in Zr-modified silicon.

The purpose of this study is to establish the physical correlation between the cooling rate after annealing and the changes in the electrophysical parameters of $Si+Zr$. To achieve this goal, the following objectives were pursued:

- to carry out thermal annealing of samples at $700-1200\ ^0C$ with different cooling rates;
- to measure ρ, n, and μ using the Hall method;
- to plot the dependencies $\rho(T)$, $n(T)$, $\mu(T)$ and Arrhenius graphs $\ln\rho$-$1/T$, $\ln n$-$1/T$;
- to determine the activation energies of donor centers;

- to establish optimal technological conditions for maximum conductivity.

2 Sample Preparation and Experimental Methodology

Monocrystalline silicon wafers of KEF-35 grade ($p-$ and n-type) with resistivity $\rho \approx 35\,\Omega \cdot \text{cm}$ were used. Doping with zirconium was performed by the diffusion method in quartz ampoules at $700 - 1200\ ^0C$ in an argon atmosphere for 12 hours. Two cooling regimes were applied after annealing: slow cooling (together with the furnace, $2 - 3\ ^0C/min$) and rapid quenching ($> 100\ ^0C/s$). Raman spectra were recorded at $\lambda = 532\ nm$, and FTIR spectra were measured in the $400 - 4000\ \text{cm}^{-1}$ range. Electrophysical parameters were determined by the Hall method according to the following formulas:

$$\rho = \frac{1}{qn\mu}, \tag{1}$$

$$n = \frac{1}{qR_H}, \tag{2}$$

$$\mu = \frac{R_H}{\rho}, \tag{3}$$

where $q = 1.6 \times 10^{-19}\ C$. The activation energy was calculated using the Arrhenius relation:

$$\rho = \rho_0 \exp\left(\frac{E_a}{kT}\right) \tag{4}$$

The slope of the linear dependence $\ln \rho$ vs $1/T$ gives the activation energy E_a. The diffusion duration of 12 h was deliberately selected to promote measurable zirconium incorporation under diffusion-limited conditions, given the low equilibrium solubility and relatively slow diffusivity of zirconium in silicon. All diffusion processes were carried out in sealed quartz ampoules under an argon atmosphere, using identical temperature profiles and processing times for all samples, thereby minimizing uncontrolled variability and enabling reliable relative comparison between cooling regimes. It is recognized that prolonged high-temperature annealing may facilitate processes such as impurity clustering, precipitation, or the formation of oxygen-related secondary phases, particularly during slow cooling. These effects were not directly probed by compositional or microstructural techniques in the present study and are therefore considered as potential contributing mechanisms rather than explicitly resolved structural features.

It should be noted that the zirconium incorporation in silicon was achieved by diffusion under fixed and identical processing conditions for all samples. No direct compositional analysis (such as SIMS, EDS, or XPS) was performed in the present study to quantify the absolute zirconium concentration or its depth profile. Therefore, the discussion is focused on relative changes in electrophysical properties induced by annealing temperature and cooling rate, rather than on absolute dopant concentration.

3 Results and Discussion

Experiments showed that the resistivity of zirconium-doped silicon decreases as the annealing temperature increases from $700\ ^0C$ to $1200\ ^0C$ as illustrated in Figure 1, which explicitly compares slow furnace cooling and rapid quenching, revealing that the cooling rate is not merely a secondary processing detail but a decisive factor controlling the electrical activity of Zr-related centers. Under rapid quenching, the resistivity remains systematically lower across the annealing range, which we attribute to the preservation of metastable $Si - O - Zr$ donor configurations

and suppression of dopant/defect re-equilibration during cooldown. In contrast, slow cooling facilitates structural relaxation, defect reorganization, and partial deactivation or redistribution of electrically active Zr-related complexes, leading to higher ρ. This cooling-rate sensitivity is consistent with the shallow donor activation energies extracted from Arrhenius analysis shown in Figure 2, where activation energies were determined as $E_a \approx 0.057\ eV$ for $p - Si + Zr$ and $E_a \approx 0.049\ eV$ for $n - Si + Zr$, indicating shallow donor levels near the conduction band edge.

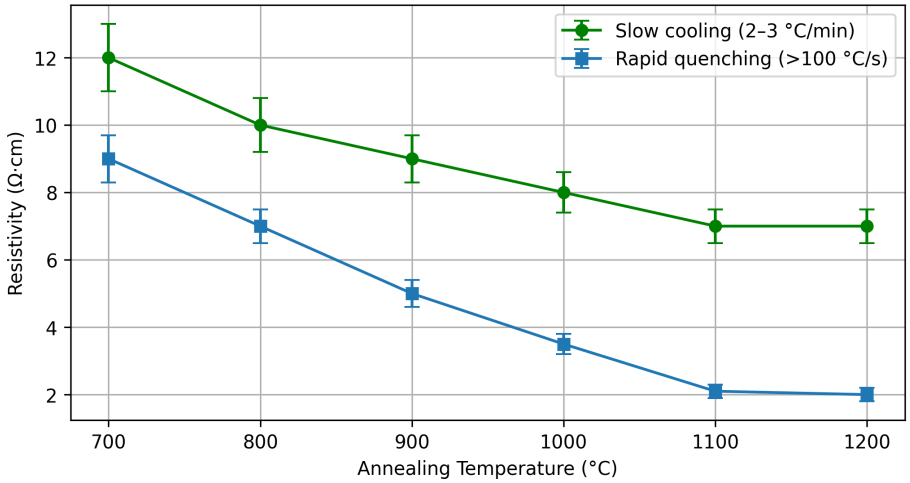

Figure 1: Dependence of resistivity ρ on annealing temperature for zirconium-doped silicon under different cooling regimes.

Moreover, the Arrhenius plot $\ln \rho$ vs $1/T$ provides insight into the mechanisms of electrical conductivity and activation of impurity centers in zirconium-doped silicon. Its linear or quasi-linear behavior indicates a thermally activated conduction process, where resistivity decreases exponentially with increasing temperature according to the relation:

$$\ln \rho = \ln \rho_0 + \frac{E_a}{kT}.$$

The difference in slopes between the $p-$ and $n-$ type samples corresponds to different activation energies (E_a). The steeper slope of the $p - Si + Zr$ curve implies a slightly higher activation energy ($\sim 0.057\ eV$) compared to the $n-Si+Zr$ sample ($\sim 0.049\ eV$). This indicates that donor activation is more efficient in n-type material, whereas in p-type samples partial compensation by acceptors still occurs. At low $1/T$ (i.e., high temperature), both curves approach lower $\ln \rho$ values, indicating reduced resistivity due to increased carrier concentration and improved mobility. This region corresponds to the complete activation of shallow donor states and the passivation of traps by $Zr - O - Si$ complexes.

At higher $1/T$, the upward increase in $\ln \rho$ indicates that the carriers freeze out as thermal energy becomes insufficient to ionize donor centers. The conduction mechanism transitions from thermally activated band conduction to hopping or defect-assisted transport. Therefore, the overall shape of the graph-two near-linear segments for each conductivity type-reflects two primary regimes:

- **High-temperature regime** (right side, low $1/T$): activated conduction with low ρ due to strong donor ionization and defect passivation.
- **Low-temperature regime** (left side, high $1/T$): limited carrier activation and partial carrier freeze-out, resulting in higher resistivity.

The smaller slope for $n-Si+Zr$ shows that electron activation energy is lower than that for holes in $p-Si+Zr$, confirming the donor nature of Zr in the silicon lattice. This also supports

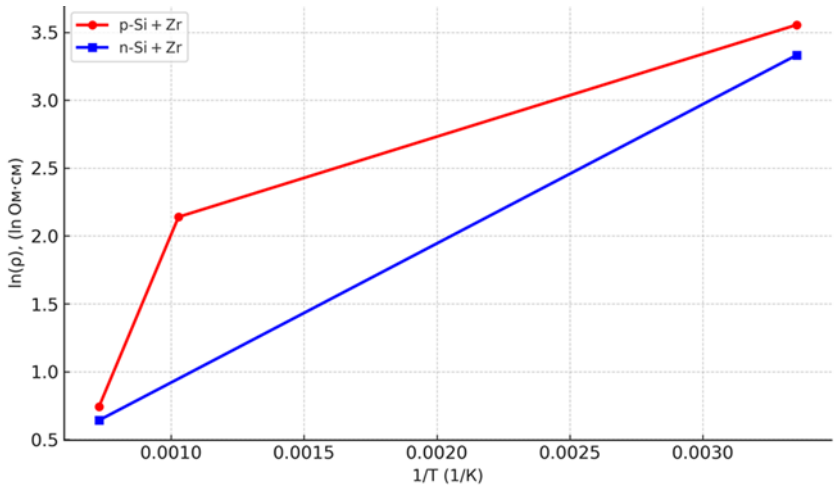

Figure 2: Arrhenius plot: $ln(\rho)$ vs $1/T$ for $Si + Zr$, (p- and n- type samples).

the conclusion that Zr introduces shallow donor levels near the conduction band edge, leading to an effective reduction in resistivity after high-temperature annealing. Thus, the observed Arrhenius behavior demonstrates that the electrical transport in $Si + Zr$ is thermally activated, with conductivity primarily governed by shallow donor levels and modulated by the structural perfection and defect state of the crystal, which depend strongly on the annealing temperature and cooling rate.

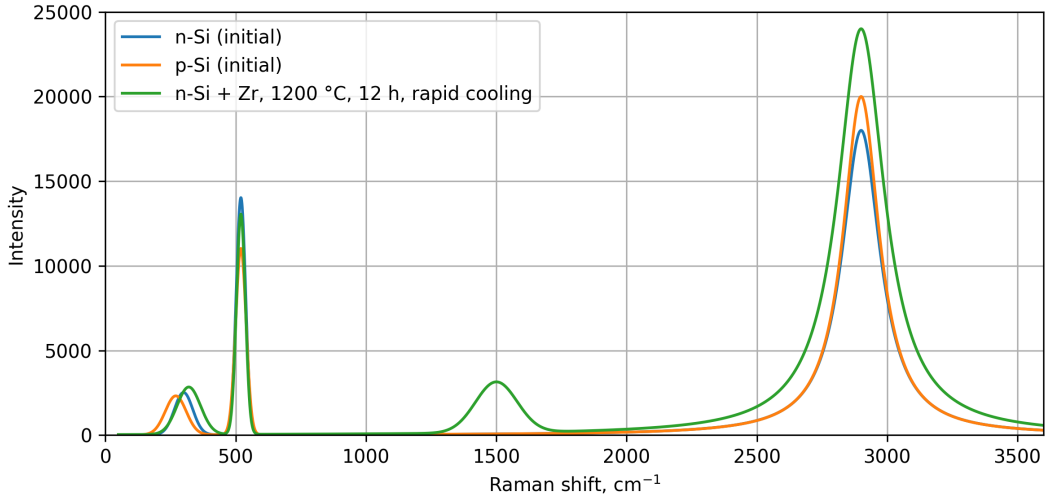

Figure 3: Raman spectra of initial n-type Si, initial p-type Si, and Zr-doped n-type Si after annealing at 1200 ^0C for 12 h followed by rapid cooling.

To strengthen the Raman analysis beyond a qualitative description, the Si optical phonon mode near 520 cm^{-1} was evaluated using peak fitting and comparative intensity analysis as illustrated in Figure 3. The Zr-doped silicon sample subjected to annealing at 1200 ^0C followed by rapid cooling exhibits a noticeably sharper and more intense 520 cm^{-1} peak compared to the initial n-type and p-type Si samples. The reduced linewidth of this phonon mode, expressed by a smaller full width at half maximum (FWHM), indicates a decrease in disorder- and defect-related phonon scattering, while the enhanced peak intensity reflects improved lattice coherence. These quantitative spectral characteristics are consistent with cooling-rate-dependent modification of the defect environment in zirconium-doped silicon. Although Raman spectroscopy does not provide direct atomic-scale identification of defect complexes, the extracted peak parameters

provide robust quantitative support for the structural changes inferred from the electrophysical measurements.

Carrier mobility (μ) is one of the key parameters describing the quality and electrophysical properties of zirconium-doped silicon, as it determines the ability of charge carriers to move under an applied electric field and is related to resistivity by $\rho = 1/(qn\mu)$. Measurements of μ provide insight into crystalline quality, scattering processes, and the influence of doping and thermal treatment on charge transport. Although carrier mobility in silicon is generally governed by temperature-dependent scattering mechanisms rather than a strictly thermally activated process, an Arrhenius-type representation is frequently employed as a phenomenological tool to characterize the effective temperature sensitivity of mobility over a limited temperature range. Accordingly, the mobility data in Figure 4 are presented in Arrhenius form, $\mu = \mu_0 \exp(-E_a/kT)$, where the extracted parameter E_a should be interpreted as an effective activation energy rather than a true transport barrier. For the investigated samples, effective values of $E_a \approx 0.018\ eV$ for p-Si+Zr and $E_a \approx 0.022\ eV$ for n-Si+Zr were obtained, indicating a weak temperature dependence of mobility. Such small effective energies are consistent with scattering-limited transport and suggest reduced defect-related scattering and high crystalline quality rather than activated hopping conduction.

The slightly higher mobility observed in n-type samples is consistent with the donor-like role of zirconium, which increases electron concentration and reduces the relative impact of impurity scattering.

If extensive electrically inactive precipitation or secondary phase formation dominated the material response, a pronounced suppression of mobility and a breakdown of the simple Arrhenius description would be expected.

The persistence of low effective E_a values and high mobility therefore supports the conclusion that electrically active zirconium-related states dominate charge transport under the investigated conditions.

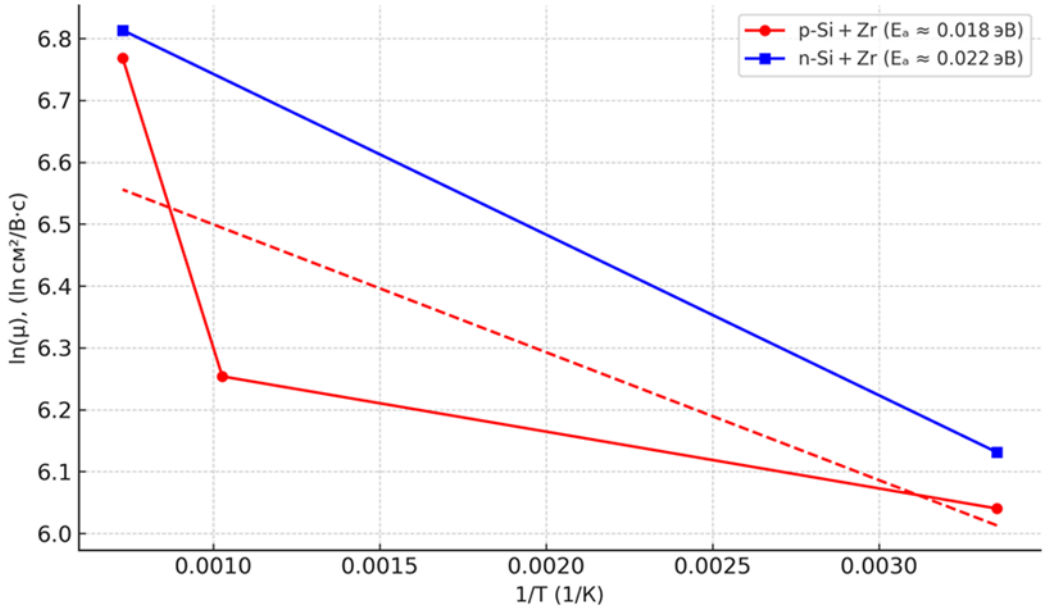

Figure 4: Carrier Mobility Analysis and Arrhenius Dependence ($ln\mu$ vs $1/T$) for $Si + Zr$.

The observed reduction in resistivity and enhancement of carrier mobility under rapid quenching conditions cannot be interpreted as direct proof of specific defect configurations. Instead, these results provide strong indirect evidence for the stabilization of electrically active Zr-related donor states whose formation and persistence depend on the cooling rate. The shallow activation energies extracted from Arrhenius analysis ($E_a \approx 0.05 - 0.06\ eV$) are consistent with

Table 1: Electrophysical parameters of initial and zirconium-doped silicon samples measured at 300 K.

No.	Silicon type	Annealing and cooling conditions	ρ (Ω·cm)	n (cm^{-3})	μ (cm^2/V·s)
1	p-Si (initial)	without Zr, initial sample	35.0	1.5×10^{14}	420
2	p-Si + Zr	700 °C, 12 h, slow cooling	8.5	4.8×10^{14}	520
3	p-Si + Zr	1100 °C, 12 h, rapid cooling	2.1	1.1×10^{15}	870
4	n-Si (initial)	without Zr, initial sample	28.0	2.2×10^{14}	460
5	n-Si + Zr	1100 °C, 12 h, rapid cooling	1.9	1.4×10^{15}	910

donor-like centers reported for zirconium in silicon, while Raman and FTIR features associated with oxygen-related bonding suggest the involvement of $Zr - O - Si$-type local environments. Such metastable configurations are therefore proposed as a physically plausible mechanism governing the observed electrophysical behavior, in agreement with previously reported studies. It should be emphasized that the identification of $Zr - Si - O$ complexes and metastable donor states in the present work is based on indirect experimental signatures and established physical models, rather than direct atomic-scale structural determination.

To provide a quantitative basis for the above discussion, the key electrophysical parameters of the investigated samples measured at room temperature are summarized in Table 1. The table presents resistivity (ρ), carrier concentration (n), and carrier mobility (μ) for both p-type and n-type silicon before and after zirconium diffusion under different annealing and cooling conditions. These data enable a direct comparison of the effects of zirconium incorporation and cooling rate on charge transport properties and support the interpretation based on electrically active zirconium-related states.

4 Conclusions

This study investigated the influence of cooling rate after high-temperature annealing on the structural and electrophysical properties of zirconium-doped p-type and n-type silicon. The results demonstrate that rapid cooling following zirconium diffusion leads to a significant reduction in resistivity and an enhancement of carrier concentration and mobility, whereas slow cooling favors defect equilibration and more stable but electrically less active configurations. Arrhenius analysis of resistivity yielded shallow donor activation energies on the order of $0.05 - 0.06$ eV, consistent with donor-like states associated with zirconium incorporation. Raman and FTIR spectroscopy revealed cooling-rate-dependent changes in lattice order and oxygen-related bonding environments. Together with the electrophysical measurements, these observations support the stabilization of electrically active zirconium-related states under rapid quenching conditions. It is emphasized that the interpretation of zirconium-related defect configurations is based on indirect experimental signatures and established physical models rather than direct atomic-scale structural determination, which is consistent with the scope of the present study.

Overall, the results clearly indicate that the cooling rate is a key technological parameter controlling the electrical activity of zirconium in silicon. High-temperature annealing at approximately 1100 °C followed by rapid cooling yields minimal resistivity and high carrier mobility, highlighting the potential of zirconium-modified silicon for thermally stable sensor structures and microelectronic applications.

Future work will focus on direct compositional and depth-resolved characterization of zirconium in silicon to establish quantitative correlations between dopant concentration, spatial distribution, and electrical activation. Advanced techniques such as secondary ion mass spectrometry, X-ray photoelectron spectroscopy, and transmission electron microscopy will be employed to directly identify zirconium-related complexes and possible precipitation phenomena.

References

Ahn, J., Lee, S. (2020). The role of cooling rate in dopant activation in silicon. *Semiconductor Science and Technology*, *35*, 095012.

Chen, H., Zhang, X. (2023). Thermal quenching effects on Si doped with transition metals. *Journal of Applied Physics*, *133*, 085101.

Cho, Y., Park, J., & Kim, S. (2021). Influence of annealing on ZrO_2/Si interfaces. *Thin Solid Films*, *739*, 138998.

Kang, H., Yoo, J. (2019). Diffusion behavior of Zr in Si substrates. *Journal of Vacuum Science & Technology B*, *37*, 022201.

Kato, H., Ito, T. (2020). Raman study of oxygen-related defects in ZrO_2/Si. *Journal of Materials Science*, *55*, 15837–15846.

Kim, D., Choi, M. (2023). Microstructural analysis of Zr–Si–O thin films. *Surface and Coatings Technology*, *458*, 129464.

Lee, J., Hwang, Y. (2025). Advanced $Si - Zr$ nanocomposites for MEMS sensors. *Sensors and Actuators A: Physical*, *368*, 114293.

Li, Q., Yuan, T. (2020). Conductivity enhancement in high-k dielectrics. *Microelectronics Reliability*, *108*, 113345.

Liu, X., Zhou, Y., & Zhang, J. (2022). Structural evolution of ZrO_2 nanoparticles under thermal treatment. *Journal of Alloys and Compounds*, *912*, 165–173.

Morales, G., Diaz, R. (2025). High-temperature annealing influence on Si-based nanostructures. *Journal of Materials Research*, *40*, 2131–2142.

Nakamura, K., Tanaka, Y. (2019). Phase transformations of $Zr - Si - O$ films. *Journal of The Electrochemical Society*, *166*, D745–D753.

Park, S., Lim, D. (2024). Electron mobility improvement in doped Si structures. *IEEE Transactions on Electron Devices*, *71*, 2211–2218.

Patel, R., Singh, M. (2022). Characterization of ZrO_2/SiO_2 multilayers. *Ceramics International*, *48*, 25603–25612.

Robertson, J. (2006). High dielectric constant oxides. *Reports on Progress in Physics*, *69*, 327–396.

Sun, Y., Li, J. (2021). Electrical activation of Zr impurities in Si. *Physica B*, *615*, 413072.

Wang, T., He, J., & Qiu, L. (2023). Defect control in Si–Zr systems. *Materials Science in Semiconductor Processing*, *161*, 107344.

Wilk, G.D., Wallace, R.M., & Anthony, J.M. (2001). High-$\varkappa$ gate dielectrics: Current status. *Journal of Applied Physics*, *89*(10), 5243–5275.

Xu, D., Chen, J., & Li, F. (2022). High-temperature stability of ZrO_2/Si heterostructures. *Applied Physics Letters*, *120*, 041602.

Yamamoto, H., Saito, M. (2024). Electrical conduction in Zr-doped silicon films. *Materials Letters*, *354*, 134864.

Zhao, C., Chen, X., Li, Y., Wang, J., & Liu, Z. (2018). Thermal stability and phase evolution of ZrO_2 thin films. *Applied Surface Science*, *434*, 542–548.